

Contribution de l'analyse thermique MBSE et 3D à la conception du moteur de l'actionneur de stabilisateur d'un avion régional

Grégoire LENOBLE^{1*}, Marie OLIVIER¹, David DONJAT², Anton STEBLINKIN³

¹Siemens PLM, LMS Engineering, 84 Quai Charles de Gaulle 69006 Lyon, France

²DMAE – UFT-MiP – ONERA, 2 Avenue Edouard Belin 31055 Toulouse, France

³TsAGI, Zhukovsky st. 1, Zhukovsky, Moscow region 140180 Russia

* (auteur correspondant : Gregoire.Lenoble@siemens.com)

Résumé - Aircraft hydraulic systems traditionally provide power for flight surface actuation, but are heavy, complex to maintain in service, and consume significant amounts of energy. Electrical based actuators help tackle these issues, but come with other challenges, such as thermal integration. Indeed, the close vicinity of several heat sources (hydraulic pump and bloc, electrical motor, control unit) in a cavity that is only passively cooled makes it difficult to guarantee the electrical motor and Electronic Control Unit (ECU) safe operation over the entire aircraft mission from a thermal point of view. In addition, systems thermal behavior can be critical when used inside composite structures that can lose durability under high temperatures. Collaborative European-Russian project RESEARCH (w3.onera.fr/RESEARCH/) has enabled the thermal analysis of a regional aircraft stabilizer bay that houses two elevator actuators, so as to support and optimize actuator motor design. This analysis largely relied on Model Based Systems Engineering (MBSE) given the early actuator design phase and the need for mission-wide analysis, through a number of varying scenarios. However the additional insight of three-dimensional analysis has also been included with simulations performed at thermally critical flight conditions. The methodology, models, outputs and implications for motor design gained from this study are described in this paper.

Nomenclature

$Abscoeff$	Surface absorption coefficient	ϵ_{gw}	Surface to air emission factor
S_d	Tube differential section (m ²)	λ	Thermal conductivity (W/m/K)
t	Time (s)	φ	Heat flux (W)
T	Temperature	η	Efficiency
V	Volume (m ³)		
W	Work (J)	Nu	Nusselt number
z	Tube stroke (m)	Re	Reynolds number
H	Altitude (m)	Ra	Rayleigh number
HTC	Convective Heat coefficient (W/m ² /K)		

1. Introduction

The reduction of fuel burn has become a priority for most aircraft operators due to environmental and cost implications. Such interest has encouraged the aerospace industry to look at ways of minimizing fuel consumption, concluding that the approach towards a more electrical aircraft, i.e. using electricity to operate the consumers, could provide some benefits. This approach tends to remove hydraulic actuators and the hydraulic systems that feed them, as they require a significant amount of maintenance effort, are heavier and consume significant amounts of energy. Additionally, this kind of electrical components allow for a higher integration of sensors for the monitoring of actuators performance and structural integrity (from a safety point of view); or achieving an improved degree of “intelligence”, improving the actuation system integration within the controlling system or aircraft.

Despite the potential benefits indicated above, such as weight reduction, increased safety and reliability, lower consumption, reduced maintenance costs, etc... electrical actuators are not fully embraced by the industry due to some of the limitations they present in their current development stage and which prevent them from being used massively or in critical areas, such as the aircraft primary flight surfaces. These limitations are: high actuator weight, safety concerns due to the jamming probability of electromechanical actuators (EMAs) and Electro Magnetic Compatibility (EMC) issues. Systems thermal behavior and integration is one of the most challenging among these issues. For this reason, and the RESEARCH program being a wide objective oriented cooperative project, the decisions was taken to also cover the task of managing the thermal integration of the actuation system under development by the consortium partners.

It's well known that the reliability of EMA or electro-hydrostatic actuators (EHA) systems for flight controls is dependent on their operating temperature. The A380 flight control EHA is a well-done example [1] as a backup actuator. But EHA and EMA constantly working in active regime need to be improved from a thermal management viewpoint, as the elimination of the classical hydraulic network imposes the need to dissipate heat generated by the actuation system (motor and ECU, and also harness) differently. The management of this thermal environment needs to develop both new cooling technologies (see [2]) and design optimization methods. This last improvement target appears as a key point when considering thermal aspects earlier in the design process.

1.1. Cavity configuration

Based on the results of weight and safety analyses of the different possible FCAS architectures performed by the RESEARCH consortium in the first project phase, the elevator control system of a regional passenger aircraft (100-seater) was chosen as the target application to be developed. The control system should consist of an EMA (under CESA's development, Spain) and EHA (under Moscow Aviation Institute (MAI) development, Russia) operating in parallel (active/active configuration) (see figure 1 with EHA configuration).

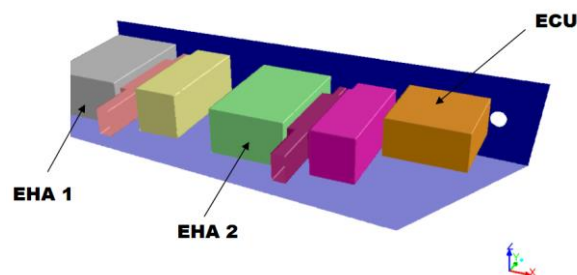


Figure 1: *Stabilizer cavity with actuating devices: EHA/EHA/ECU (ONERA)*

The overall idea was to optimize the actuators design in terms of acceptable heat losses and the heat dissipation taking into account the actuator real duty cycle and cavity geometry at the early design stage.

1.2. The flight mission

The methodology of the actuation system thermal behavior analysis described further implies the wide use of simulation, which as a first step was represented by the simulation of the cavity system thermal behavior modeled in LMS Amesim during the typical flight of a regional jet. The flight scenario is based on the real flight record and contains the data arrays of elevator actuator displacement and external forces under hinge moments as well as other flight parameters (altitude, true air speed etc.), which thus fully determines the actuation

system heat losses and heat dissipation processes. Also in order to obtain the duty cycle of the actuators during some highly loaded flight scenario, a «virtual» aircraft flight-record was also developed. It contains the influence of predefined turbulence according to Figure 2. This scenario also includes some special maneuvers during flight (e.g. s-maneuver just before landing) to put the actuation system into the most critical regime.

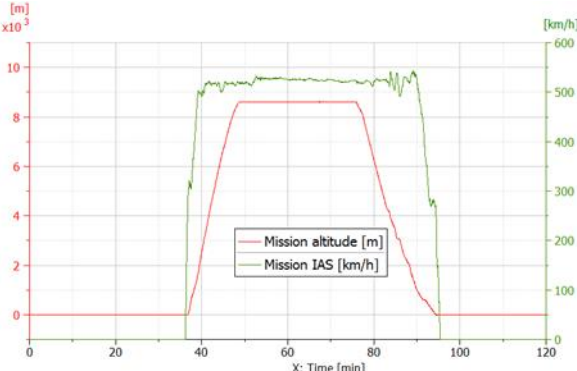


Figure 2 : «Virtual» highly loaded flight scenario

2. Thermal analysis

2.1. MBSE cavity model

2.1.1. Cavity boundary conditions

The elevator actuator operates inside a given thermal context, which will interact with the actuator bay, and even influence its thermal behavior. The following interfaces to the actuator are considered: outside air, Sun radiation, cavity structure. Outside airflow provides a large cooling effect to the cavity outside shell. This is captured both on the top and bottom panels, assuming airflow over a horizontal flat plate configuration (see Figure 3). Depending on the flight regime and air properties, forced and free convections are calculated with laminar or turbulent equations [3].

In order to ensure a smooth mathematical model over the entire range of convection regimes (purely free, mixed, purely forced), a unique Nusselt number combines the free and forced ones, so that a unique convection Heat Transfer Coefficient (HTC) can be calculated as per (1).

$$HTC = (Nu * \lambda) / L \tag{1}$$

In this outside convection case, the characteristic dimension L is the total stabilizer outside area (top and bottom) divided by its perimeter.

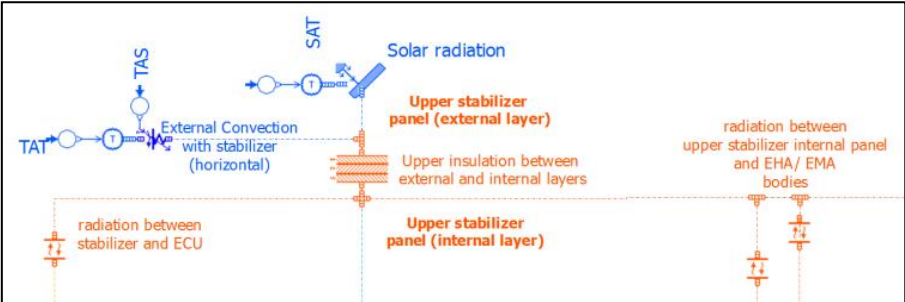


Figure 3 : Cavity top panel

Note that the air viscosity, thermal conductivity, specific heat, density and speed are dynamically updated during the aircraft mission simulation.

As shown with Figure 3, Sun radiation onto the stabilizer cavity is accounted for with (2), where θ is the angle between the cavity surface (normal vector) and the Sun direction (set to 0° so as to consider maximum Sun radiation), and *abscoeff* stands for the surface absorption factor.

$$\varphi_{Solar\ panel} = \varphi_{solar} \times \cos \theta \times area \times abscoeff \quad (2)$$

This Sun radiation is complemented with the radiative exchange the surface has with outside ambient air, as per (3), and using ε_{gw} as the outside air and cavity panel emission factor.

$$\varphi_{rad} = \sigma \cdot \varepsilon_{gw} \cdot area \cdot (T_{surface}^4 - T_{air}^4) \quad (3)$$

Note that equation (3) is a particular case of the general radiation equation that assumes an infinite “radiating air surface” and thus a view factor of 1.

As shown with Figure 4, ground radiation is accounted for in a very similar way, only with no exposure angle factor, a different ε and the ability for it to be turned off when the aircraft has left ground.

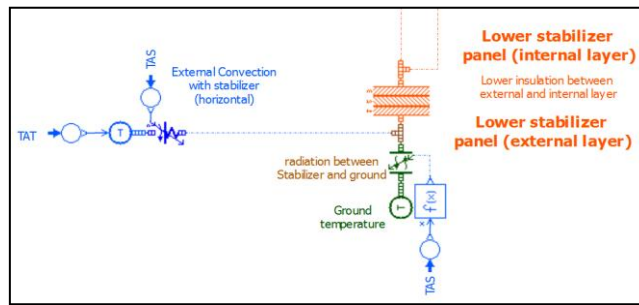


Figure 4 : Cavity bottom panel

The thermal behavior of the cavity that houses the stabilizer actuator has been simplified to that of a few panels: a vertical, and two horizontal ones: top and bottom. Top and bottom panels are the aggregate of an external layer (exposed to the Sun / ground and outside air), and an internal layer (in contact with internal air), separated by an insulation composite material, as shown with Figure 3 and Figure 4.

Finally, thermal conduction occurs from the top to the bottom panels, through the vertical one. This is captured with two instances of a “thermal conduction” component, that derive the heat flux between two solid material pieces 1 and 2; depending on is their contact surface, and contact thermal resistance. It predicts T1 and T2 temperatures, both taken at a distance d1 and d2 inside each material piece.

2.1.2. Cavity internal heat loads

The end objective of this analysis being the thermal integration of all heat sources and exchanges inside this cavity, each heat source has then been modeled individually. The heat transfer modes involved in all of the following heat loads are all based on standard heat transfer equations: free and forced convection over a flat plate, radiation in an enclosure, and linear conduction between two pieces of different material.

In this article, we are focusing on EHA systems which are modeled with a focus on their thermal interaction with the cavity. The EHA heat flux generated as a function of its duty cycle is obtained from the EHA Simulink-model developed by MAI, and split over the EHA

parts: body, motor, pump, piston and reverse valve. The EHA parts are in obviously contact, and bolted to the cavity bottom (lower panel). They dissipate EHA heat losses through conduction (to themselves, and the lower panel), forced oil convection (driven by duty cycle oil consumption), as well as air convection (forced and free) and radiation, as will be described in the next section.

The Electronic Control Unit (ECU) adds an additional third heat load into the cavity, through its thermal losses. This is captured with a single thermal capacitance. Its heat load is calculated based on the power it provides to the EHA motor, and its own efficiency η . The ECU is in thermal contact with the lower panel, and is cooled by air convection and radiation.

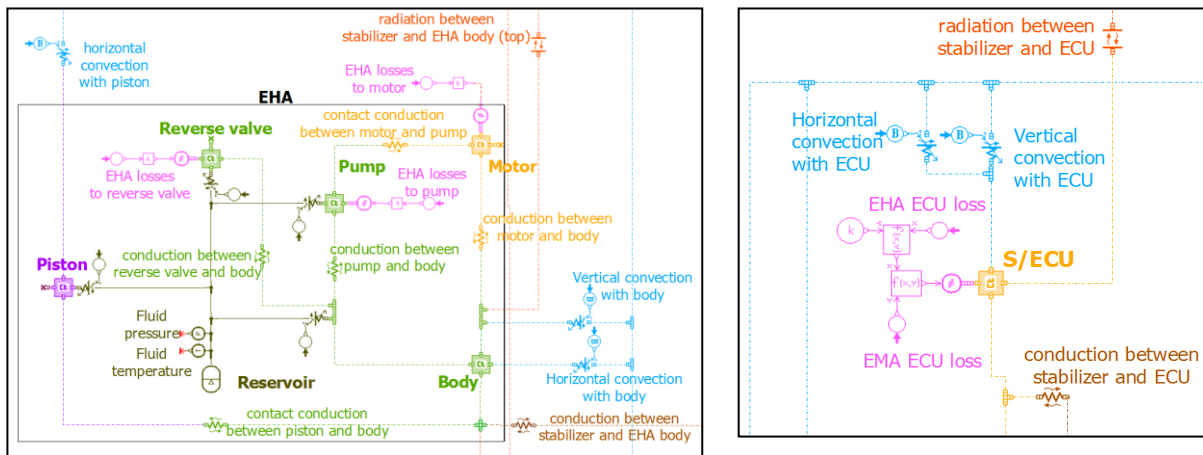


Figure 5. EHA model (left) and ECU model (right)

2.1.3. Cavity thermal integration

Thermal integration of the components described in the above sections is mostly piloted by the cavity internal convection and radiation. First, internal convection thermally connects all cavity elements: EHA / EHA, ECU and cavity panels. As seen with Figures 4 and 5, convection is modeled over “horizontal” and “vertical” faces, so as to capture all heat exchanges, distinguishing between the EMA cylindrical body and its flat end faces for example. Natural and forced convections are calculated following equations given in [3] with the additional subtlety that convection is piloted from the airspeed point of view.

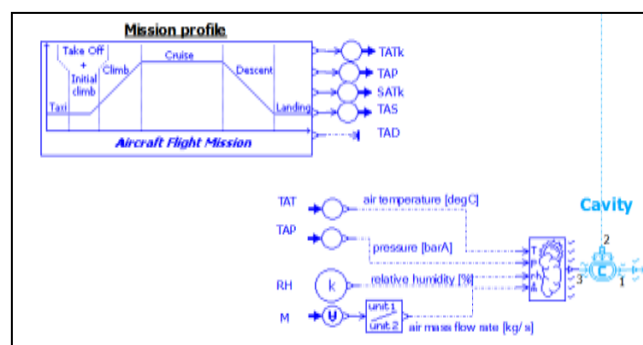


Figure 6 : Cavity model focus

LMS Amesim being a Systems Engineering tool, 2D or 3D airspeed maps cannot be predicted. Rather, this air speed information is extracted from ONERA predictions, and condensed into speed profiles that are driven by the ingested airflow, or artificially set to a minimum of 0.2 m/s in the worst case assumption of a sealed cavity, as recommended in [4]. Internal radiation completes the list of cavity internal heat exchanges, and has been allowed between all bodies (EHA, ECU) and both cavity horizontal panels. Radiations between body and from a panel to the other have been neglected given temperature levels and relative

influence with regards to convection or conduction. Finally, all heat loads, heat storage, and heat exchanges are resolved in the Cavity submodel shown in Figure 6. This submodel computes the cavity temperature and Pressure based on mass and energy conservation, respectively owing from airflows (ingested and leaked), and the heat exchanges detailed above.

3. CFD cavity model

CFD model is based on a 3D discretization of the stabilizer cavity as shown on Figure 1. Calculations are performed with FLUENT14's unsteady incompressible solver. According to our estimation of flow conditions, laminar approach is selected. For thermal problem, both free convective and radiative behaviours are resolved. For radiative approach, S2S method is preferred for 3D enclosed configuration. Boundary conditions are extracted from LMS Amesim software simulation in term of heat loads (i.e. heat power released by electric items) and external airflow (i.e. SAT (or Static Air Temperature), altitude and Mach number).

4. First results

4.1. MBSE model results

The evolution of the temperature of the active EHA over the whole flight mission is shown with Figure 7. As expected, all temperatures clearly increase during both ground phases as a result of medium to high SAT and low aircraft speeds. On the opposite, low outside temperatures and high aircraft velocities during cruise directly help reduce EHA temperatures. The steeper temperature rise during approach and landing than during takeoff is a direct consequence of the quick decrease of external heat convection following landing. The temperature profiles observed for the EHA pump and motor are both higher than that of other EHA parts, but yet exhibit different time variations. This is explained by the fact that they both reject the same thermal power (approx. 30W), but have different weights (as summarized with Table 1), which results in different heat per unit mass values.

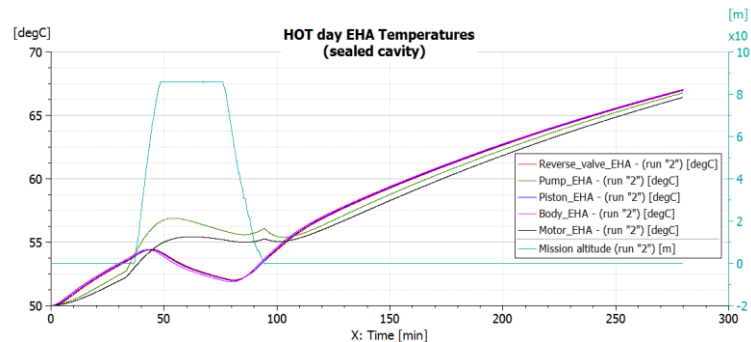


Figure 7. Time profiles of the active EHA lumped temperatures on HOT days, for a sealed cavity (no air ingestion)

The watchful reader may observe that the flight mission shown with Figure 2 has been extended by 160mins in the taxi-in phase. Although highly unrealistic, this was done so as to verify long-term temperature stabilizations, and made possible by the very low CPU run times of the LMS Amesim software model (100 CPU s for 16800s simulated). Despite this mission extension, all temperatures keep rising after landing and taxi-in phases, even with moderate heat release levels (6W for the EHA, and 20W for the ECU). This can be explained with the conservative assumption of a sealed cavity, combined with a low wind speed assumption (1 m/s) that do not provide sufficient cooling to the cavity and its actuators. This behavior does not hold when cavity ventilation is introduced, as described in section “EMA design support”. The results shown above have confirmed that, as expected, the flight condition that is most

critical and demanding from a thermal point of view is the landing / taxiing phase. Therefore, it has been decided to further analyze the cavity thermal behavior straight after landing ($t=95\text{min}$) with the CFD model described previously. The end of cruise condition ($t=76,7\text{min}$) has also been analyzed, given that it is the operating point where actuators are designed to operate for the longest part of their life.

4.2. CFD model results

The temperatures of the cavity bodies obtained from CFD analysis in an EHA-EHA configuration, on a HOT day, in steady state conditions, are given below as body averages to allow for a comparison with MBSE results (extracted from Figure 7). End of cruise conditions ($t=76,7\text{min}$) are given and compared with MBSE results in Table 1.

Temperature (°C)	CFD	MBSE	Δ
Mean EHA	51.9	54.3	5%
ECU	47	52.4	11%
Cavity	15.1	45	198%
Upper panel -internal	--	35.6	--
Upper panel -external	-3	-4	33%

Table 1. *Time profiles of the active EHA lumped temperatures on HOT days, for a sealed cavity (no air ingestion)*

CFD	MBSE	Δ
52	54.9	6%
63.2	55.8	12%
53.2	53.6	1%
--	53.2	--
50	50	0%

Table 2. *CFD averaged temperatures, steady state at landing conditions, sealed cavity, HOT day, $\epsilon=0.9$*

Interpretation of the MBSE and CFD results provided in Table 1 is of great interest, providing average differences around 6 to 7% for the values that should be compared, 5% as a minimum discrepancy, and 11% as a maximum one. The main contributors to these discrepancies are believed to be differences in local HTC values, and radiation view factors. In this result post-processing summary percentages, the CFD cavity temperature at End of Cruise is not included, as it clearly highlights a limitation to the current model. This is believed to be linked to the inaccurate accounting of thermal conduction along the cavity walls, currently modelled with the “shell-conduction” approach that uses an artificial meshing based on the real panel thicknesses. Improvements to this approach are currently being investigated. Also left out of the post-processing summary percentages is the cavity upper panel external temperature since the end of cruise difference is 1degC only, but also since solar radiation is not yet accounted for in the CFD model. This will be added in future versions of the model, given its importance when compared with other heat fluxes into the cavity roof, as understood from the MBSE model (250 to 350W, compared to 200W for external convection). Keeping in mind the added value of the CFD model for an accurate prediction of radiation view factors, an additional run has been performed with the CFD model, increasing all emissivity values to $\epsilon=0.9$ (starting from 0.5 for the glass fiber and aluminum, and 0.8 for the carbon fiber). This additional CFD run provides further understanding of the cavity thermal behavior, and especially of the importance of internal radiation, which increases all internal temperatures by 2-3 °C. Just like the cavity air temperature discrepancy, this variation as a result of additional radiation can be explained with the “shell conduction” model that needs improving. Indeed, in the previous ($\epsilon=0.5$) run, inaccurate thermal conduction between the EHA constituents prevented realistic spread of the heat dissipated by the motor and pump. The rise in radiation ($\epsilon=0.9$) reduces this isolation of heat in one EHA constituent only (mostly the pump), and allows for heat propagation to the rest of the cavity and hardware. Apart from conduction and solar radiation to be refined in the CFD model, this results comparison still validates the discretization assumptions made in the MBSE analysis,

with the split of EHA actuators into a few bodies only. This is of great importance, as it gives confidence in further use of the MBSE model, whose flexibility and fast simulation capability are instrumental at this early stage of actuator design. Finally, further understanding of the flow physics at stake in the cavity is provided with Figure 9, which shows the temperature-colored profile of some cavity air flow. This illustration is key to the understanding of the natural convection happening within the cavity. A specific post-treatment will be designed during further work to post-process this information for the update (improvement) of HTC estimations used in LMS Amesim software model, basing them on local air velocities as influenced by the cavity 3D geometry rather than lumped estimates.

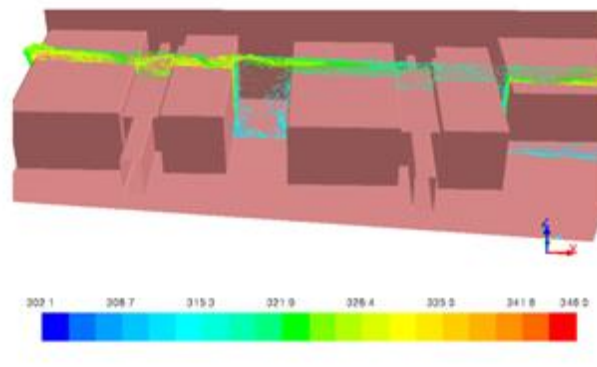


Figure 9. Cavity airflow profile colored by air temperature, HOT day, sealed cavity, taxi-in conditions

5. Conclusions

The proposed methodology obviously gives the opportunity to take into account such a critical aspect for More Electrical Aircraft (MOA) applications as system thermal behavior at the early design stage. As a result, it leads to the reduction of the systems development time and what's probably more important the output product is able to represent the more effective solution in terms of mass and dimensions leading to the reduction of the aircraft lifecycle costs. In addition the methodology used gives the ability to all the project partners to fit the outputs of their work all together on the common LMS Amesim language while focusing on their own area of expertise.

It also should be noted that several further research activities planned to become the logical continuation of the work described in the paper as the analysis of actuation system thermal behavior during highly loaded / emergency flight scenarios with turbulence and different failures and also the experimental validation of the thermal model developed in LMS Amesim and 3D calculations from ONERA. The validation is planned to be done in TsAGI with the use of the full-scale composite stabilizer and the real actuators installed inside the cavity.

References

- [1] Van Den Bossche D., "The A380 flight control electrohydrostatic actuators, achievements and lessons learnt", ICAS 2006.
- [2] Lawson, C.P., Pointon, J., "Thermal Management of Electromechanical Actuation On An All-Electric Aircraft", 26th ICAS Congress, Anchorage, Alaska. 14-19 Sept. 2008.
- [3] Incropera F.P., DeWitt D.P., (2002) *Fundamentals of Heat and Mass Transfer, fifth edition*, Jhon Wiley & Sons, Inc
- [4] Saury D, Rouger N, Djanna F, Penot F, (2009), Mesures de vitesse, de température et de flux thermique en convection naturelle en espace confiné, CONGRES SFT 2009, May 2009, Vannes, France. 1, pp.129-134, 2009.